Mouse neurexin-1α deletion causes correlated electrophysiological and behavioral changes consistent with cognitive impairments

Mark R. Etherton[a,1], Cory A. Blaiss[b,1], Craig M. Powell[b,c], and Thomas C. Südhof[a,d,e,f,g,2]

[a]Department of Molecular and Cellular Physiology and [d]Howard Hughes Medical Institute, Stanford University, 1050 Arastradero Road, CA 94304; and Departments of [b]Neurology, [c]Psychiatry, [e]Neuroscience, and [f]Molecular Genetics, and [g]Howard Hughes Medical Institute, University of Texas Southwestern Medical Center, Dallas, TX 75390

Contributed by Thomas C. Südhof, September 9, 2009 (sent for review August 2, 2009)

Deletions in the neurexin-1α gene were identified in large-scale unbiased screens for copy-number variations in patients with autism or schizophrenia. To explore the underlying biology, we studied the electrophysiological and behavioral phenotype of mice lacking neurexin-1α. Hippocampal slice physiology uncovered a defect in excitatory synaptic strength in neurexin-1α deficient mice, as revealed by a decrease in miniature excitatory postsynaptic current (EPSC) frequency and in the input-output relation of evoked postsynaptic potentials. This defect was specific for excitatory synaptic transmission, because no change in inhibitory synaptic transmission was observed in the hippocampus. Behavioral studies revealed that, compared with littermate control mice, neurexin-1α deficient mice displayed a decrease in prepulse inhibition, an increase in grooming behaviors, an impairment in nest-building activity, and an improvement in motor learning. However, neurexin-1α deficient mice did not exhibit any obvious changes in social behaviors or in spatial learning. Together, these data indicate that the neurexin-1α deficiency induces a discrete neural phenotype whose extent correlates, at least in part, with impairments observed in human patients.

autism | neuroligin | schizophrenia | synaptic cell-adhesion | synapse

Neurexins are neuronal cell-surface proteins that were identified as receptors for α-latrotoxin, a presynaptic toxin that triggers massive neurotransmitter release (1–3). Neurexins are largely presynaptic proteins that form a transsynaptic cell-adhesion complex with postsynaptic neuroligins (4, 5). Vertebrates express three neurexin genes, each of which includes two promoters that direct the synthesis of the longer α-neurexins and the shorter β-neurexins (6, 7). Neurexins are expressed in all neurons, and are subject to extensive alternative splicing, generating >1,000 splice variants, some of which exhibit highly regulated developmental and spatial expression patterns (8).

The properties of neurexins suggested that they function as synaptic recognition molecules (1), and mediate transsynaptic interactions via binding to neuroligins (4). In support of this overall concept, α-neurexin triple KO mice exhibit major impairments in synaptic transmission that manifest largely, but not exclusively, as presynaptic changes (9–13). Importantly, α-neurexin KO mice do not display a major decrease in the number of excitatory synapses, and only a moderate decrease in inhibitory synapses (9, 13). Thus, neurexins appear to be essential components of synaptic function whose roles extend to several different components of synapses.

In recent years, enormous progress in human genetics has led to the identification of multiple genes that are linked to autism spectrum disorders (ASDs) and schizophrenia. Interestingly, copy-number variations in the neurexin-1α gene (but not the neurexin-1β gene) were repeatedly observed in patients with ASDs (14–21) and schizophrenia (22–25). Because 0.5% of all ASD cases appear to harbor neurexin-1α gene deletions, and ASDs are highly prevalent, thousands of ASD patients carry neurexin-1α deletions. Thus, understanding the biology of neurexin-1α and its role in the pathogenesis of ASDs and schizophrenia assumes added importance. In view of the human clinical genetics data, we have now performed an in-depth analysis of the synaptic phenotype produced by the neurexin-1α deletion in mice, and examined the behavioral consequences of this deletion. Based on the viability of neurexin-1α KO mice and on the human condition, we expected a limited phenotype without incapacitating impairments. Indeed, our data show that neurexin-1α KO mice exhibit a discrete, but significant, electrophysiological phenotype that is associated with pervasive behavioral abnormalities, which in turn, are suggestive of some features of cognitive diseases.

Results

Deletion of Neurexin-1α Reduces Spontaneous Excitatory Synaptic Transmission. We first used whole-cell voltage-clamp recordings to measure spontaneous miniature excitatory postsynaptic currents (mEPSCs) and miniature inhibitory postsynaptic currents (mIPSCs) in hippocampal CA1 pyramidal neurons in the presence of TTX (Fig. 1 *A–C*). Neurexin-1α KO mice exhibited a significant, and selective, decrease in mEPSC frequency without a change in mIPSC frequency, indicating a potential impairment in excitatory synaptic transmission or excitatory synapse number (Fig. 1*B*). Also, no change in the mEPSC or mIPSC amplitude was observed, which suggests that deletion of neurexin-1α did not alter the quantal size or postsynaptic receptor numbers (Fig. 1*C*).

To further test the effect of neurexin-1α deletion on spontaneous neurotransmission, we assessed the excitatory/inhibitory balance of individual neurons in the CA1 region of the hippocampus. Specifically, we used whole-cell voltage-clamp recordings to monitor spontaneous miniature events in the same neuron both at the chloride-reversal potential (−60 mV; to measure mEPSCs) and at the glutamatergic current reversal potential (0 mV; to measure mIPSCs) in artificial cerebrospinal fluid containing only TTX. Using this approach (Fig. 1 *D–F*), we confirmed that neurexin-1α KO neurons exhibited a reduced mEPSC frequency that resulted in a shift in the excitatory/inhibitory balance of individual CA1 pyramidal neurons to favor decreased excitatory input. In summary, these findings suggest that deletion of neurexin-1α impairs excitatory synaptic transmission in the hippocampus.

Author contributions: M.R.E., C.A.B., C.M.P., and T.C.S. designed research; M.R.E. and C.A.B. performed research; M.R.E., C.A.B., C.M.P., and T.C.S. analyzed data; and M.R.E., C.A.B., C.M.P., and T.C.S. wrote the paper.

The authors declare no conflict of interest.

[1]M.R.E. and C.A.B. contributed equally to this work.

[2]To whom correspondence should be addressed. E-mail: tcs1@stanford.edu.

This article contains supporting information online at www.pnas.org/cgi/content/full/0910297106/DCSupplemental.

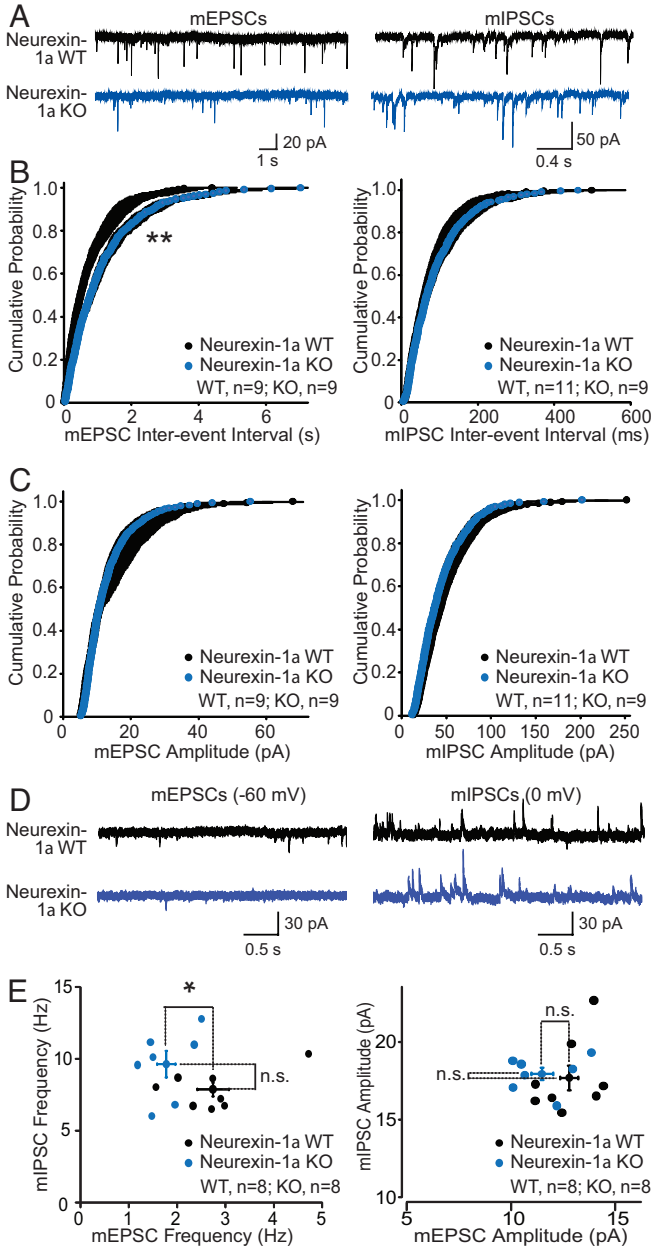

Fig. 1. Neurexin-1α KO mice exhibit a reduced mEPSC frequency in the CA1 region of the hippocampus. (*A*) Representative traces of mEPSCs (*Left*) and mIPSCs (*Right*) recorded in hippocampal CA1 pyramidal neurons in the presence of 0.5 μM TTX with a high-chloride (mIPSCs) or methanesulfonate (mEPSCs) internal pipette solution. (*B* and *C*) Cumulative distributions of the interevent intervals (*B*) and amplitudes (*C*) of mEPSCs (WT, nine cells per three mice; KO, nine cells per three mice) (*Left*) and mIPSCs (WT, 11 cells per three mice; KO, nine cells per three mice) (*Right*). Statistical significance was assessed with a Kolmogorov–Smirnov test (**, $P < 0.01$). (*D* and *E*) Representative traces (*D*) and summary graphs (*E*) of sequential measurements of the frequency and amplitudes of mEPSCs (*Left*) and mIPSCs (*Right*; monitored at −60 and 0 mV holding potentials, respectively) in the same pyramidal CA1 neuron (WT, eight cells per three mice; KO, eight cells per three mice). Recordings were obtained with a modified methanesulfonate internal pipette solution. Representative traces are depicted on top, and summary plots with each cell represented by a dot on the bottom. Means ± SEMs are indicated by the cross symbols; statistical significance was evaluated with Student's *t* test (*, $P < 0.05$; ns, nonsignificant).

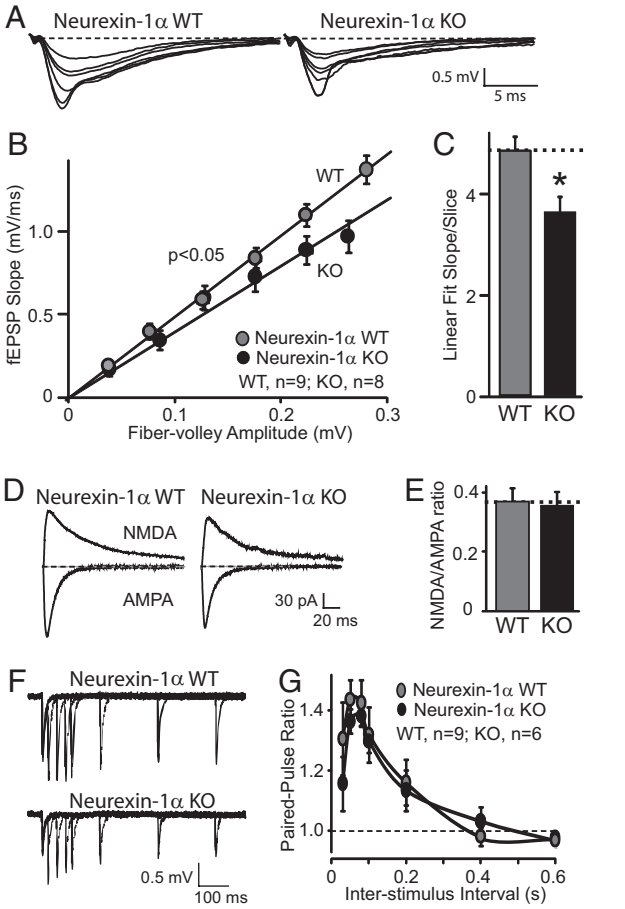

Fig. 2. Neurexin-1α KO mice exhibit a decrease in excitatory synaptic strength in the CA1 region of the hippocampus. (*A*) Sample traces for extracellular field EPSP recordings performed in stratum radiatum of CA1 region of hippocampus. (*B*) Summary graph of input-output measurements. The slope of the fEPSP is plotted as a function of the fiber-volley amplitude (WT, three mice per nine slices; KO, three mice per eight slices). Linear fit slopes were calculated for WT (4.815 ± 0.285) and KO (3.616 ± 0.296) slices and were significantly different ($P = 0.011$, unpaired Student's *t* test). (*C*) Summary graph of linear fit slopes for WT and KO input-output curves. (*D* and *E*) Sample traces and summary graph for whole-cell voltage clamp recordings of NMDA/AMPA ratio in CA1 pyramidal neurons (WT, three mice per six cells; KO, three mice per eight cells). (*F* and *G*) Sample traces and summary graph for paired-pulse facilitation measurements (fEPSP2/fEPSP1) recorded at various interstimulus intervals (WT, three mice per nine slices; KO, three mice per six slices). Data represent means ± SEM.

Neurexin-1α KO Mice Exhibit Decreased Evoked, Excitatory Synaptic Strength in Area CA1 of the Hippocampus. To test whether the decreased mEPSC frequency corresponds to a decrease in synaptic strength, we recorded evoked field excitatory postsynaptic potentials (fEPSPs) in acute slices from the CA1 region of the hippocampus. Consistent with the mEPSC findings, we observed a significant decrease in the input-output relationship of excitatory synaptic transmission in neurexin-1α KO slices (Fig. 2 *A*–*C*), suggesting that there is a decrease in basal excitatory synaptic strength. Measurements of the fEPSP response to paired stimuli at various interstimulus intervals showed that the paired-pulse ratio (fEPSP2/fEPSP1) was similar in neurexin-1α KO and WT control slices (Fig. 2 *F* and *G*). Also, we monitored the ratio of NMDA- and AMPA-receptor mediated synaptic currents. To measure the ratio of NMDA- vs. AMPA-receptor mediated synaptic currents, we performed whole-cell voltage-clamp recordings at a holding potential of −70 mV to measure evoked monosynaptic AMPA-receptor mediated responses, and at a holding potential of +40 mV to measure NMDA-receptor mediated responses. For the latter,

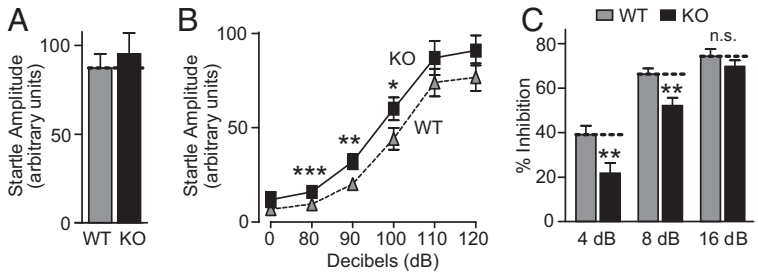

Fig. 3. Neurexin-1α KO mice exhibit impaired PPI. (*A*) Mean startle amplitude to an initial 120 dB sound pulse (repeated six times). (*B*) Startle responses to eight presentations of the following sound pulses (presented in pseudorandom order): no stimulus, 80, 90, 100, 110, and 120 dB pulse. For each pulse, the mean startle amplitudes were averaged. (*C*) PPI measurements, performed in mice randomly exposed to five trial types: pulse alone (120 dB), three different prepulse/pulse pairings [prepulses at 4, 8, or 16 dB above the background noise (70 dB), followed by a 120 dB pulse with a 100-ms onset-onset interval], and no stimulus. Data show the percentage inhibition of the mean startle amplitude. Data shown are means ± SEMs (*, $P < 0.05$; **, $P < 0.01$; and ***, $P < 0.001$ compared with WT; for a full description of statistical tests and results, see *SI Appendix*).

the amplitude 50 ms poststimulus was used to avoid contamination with AMPA-receptor mediated currents (see *Methods*). Again, we detected no abnormality in neurexin-1α KO mice, suggesting that the impairment in synaptic strength is not due to a postsynaptic receptor-dependent mechanism.

Neurexin-1α KO Mouse Behavior Exhibits Impaired Prepulse Inhibition (PPI). Because patients with both ASDs and schizophrenia display impaired PPI (26–28), we hypothesized that neurexin-1α KO mice may also have this phenotype. To test this hypothesis, we first measured acoustic startle reactivity during initial presentations of a 120-dB auditory pulse (the baseline startle amplitude), and the difference between genotypes was not statistically significant (Fig. 3*A*; for detailed description of all statistical results, see *SI Appendix*). However, when we monitored the acoustic startle reactivity in response to lower-intensity auditory stimuli (80–120 dB), we detected a small, but statistically significant, enhancement of the startle response to stimuli of 80–100 dB (Fig. 3*B*).

In the next set of experiments, we measured actual PPI, which consists of the inhibition of the startle response induced by a 120-dB pulse preceded by a low-level acoustic stimulus (26–28). Compared with WT mice, neurexin-1α KO mice exhibited significantly decreased PPI at low prepulse levels (≈45% decrease at 4 dB; Fig. 3*B*). This decrease in PPI was not due to a decrease in the startle response or acoustic perception, because, as shown above, neurexin-1α KO mice were slightly more, and not less sensitive, to acoustic stimuli at lower levels (Fig. 3*B*). There was no difference in body mass between the genotypes ($P = 0.66$) that could confound the measurement of startle responses. The changes in PPI and startle threshold observed here, while nonspecific, indicate impairments in sensorimotor gating (29, 30), consistent with abnormal circuit function in the central nervous system of the neurexin-1α KO mice.

Neurexin-1α KO Mice Exhibit Increased Repetitive Grooming Behaviors. Because "restricted repetitive and stereotyped patterns of behavior" are one of the core diagnostic criteria of autism (31), we next examined self-grooming, a stereotyped behavior in mice. Neurexin-1α KO mice spent almost twice as much time grooming themselves as littermate WT mice (Fig. 4*A*). This increase in total time spent grooming was due to a significant increase in the frequency of grooming bouts (Fig. 4*B*), and associated with a nonsignificant increase in the time spent grooming per bout (Fig. 4*C*).

Neurexin-1α KO Mice Display No Abnormalities in Social Behaviors. Because impairments in social behaviors are a hallmark of ASDs (31–34), we examined social behaviors and social learning in neurexin-1α KO mice. However, although we used four different social interaction paradigms, we detected no abnormalities (see *SI Appendix*). Because normal social interactions depend on successful detection of pheromones and other olfactory cues, it is important to note that olfaction was normal in both WT and neurexin-1α KO mice. In a test of pheromone perception, mice were exposed to a slide covered with the anogenital scent of a novel adult conspecific mouse, but again there was no difference between genotypes ($P = 0.37$; *SI Appendix*). Also, during a buried food finding test, mice of the two genotypes displayed the same latency in finding a buried peanut butter cookie ($P = 0.76$; *SI Appendix*).

Neurexin-1α KO Mice Exhibit Impaired Nest-Building Behaviors. Although it is not an example of social interaction, nest building in rodents is relevant to social and/or parental behaviors (35, 36). To examine nest-building behaviors, mice were given nesting material, and the dimensions of their nests were measured over 1.5 h. When the nest width was measured, neurexin-1α KO mice showed a dramatic impairment in nest building compared with WT (Fig. 5). Specifically, the width of nests built by WT mice increased significantly over time, but the width of nests built by neurexin-1α KO mice did not increase at all (Fig. 6*A*). The nest height, in contrast, was not significantly different between mice of the two genotypes (Fig. 5*B*).

Neurexin-1α KO Exhibit Normal Anxiety-Like Behaviors, Locomotor Activity, and Spatial Learning. Because KO mice lacking the neurexin-binding partner neuroligin-2 exhibit increased anxiety (37), we examined anxiety-related and locomotor behaviors in

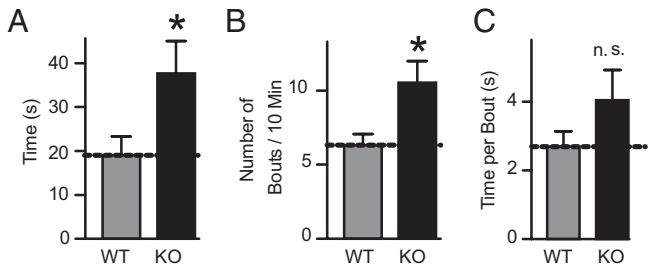

Fig. 4. Neurexin-1α KO mice exhibit increased grooming behavior. Mice were habituated in an empty cage without bedding, and grooming of all body regions was monitored for 10 min. (*A*) Mean time spent self-grooming. (*B*) Mean number of grooming bouts. (*C*) Mean time spent per grooming bout. Data shown are means ± SEMs (*, $P < 0.05$; ns compared with WT; for a full description of statistical tests and results, see *SI Appendix*).

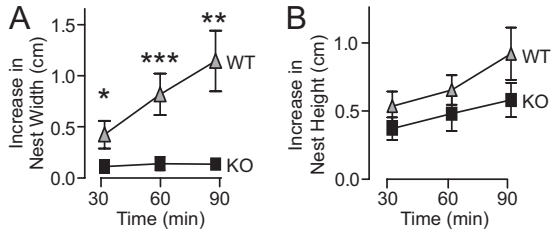

Fig. 5. Neurexin-1α KO mice exhibit impaired nest-building behaviors. (*A* and *B*) Mice were habituated in an empty cage for 15 min, and a 5 × 5 cm square of pressed cotton was placed in a random cage corner. The width (*A*) and height (*B*) of the nest built by the mouse, with subtraction of the original width and height of the cotton pad, was measured at 30, 60, and 90 min. Data shown are means ± SEMs (*, $P < 0.05$; **, $P < 0.01$; and ***, $P < 0.001$ compared with WT; for a full description of statistical tests and results, see *SI Appendix*).

neurexin-1α KO mice, but detected no significant phenotype (*SI Appendix*).

Some ASD patients with neurexin-1α mutations have IQ levels low enough for the patients to be classified as mentally retarted (15). Conversely, a dominant mutation in the postsynaptic neurexin-binding partner neuroligin-3 (R451C) enhances spatial learning in mice (38). Therefore, we examined spatial learning in neurexin-1α KO mice using the Morris water maze experiment. However, we detected no major changes in neurexin-1α KO mice during either the Morris water maze experiment or a visible platform control task (*SI Appendix*).

Neurexin-1α KO Mice Exhibit Enhanced Motor Learning on the Rotarod. In a final set of experiments, we tested motor learning in neurexin-1α KO mice on the accelerating rotarod. Neurexin-1α KO mice displayed normal motor coordination during the initial trials, but exhibited enhanced motor learning compared with WT mice as the trials continued (Fig. 6*A*). By the tenth trial, the neurexin-1α KO mice had become so proficient that several of them were able to remain on the rotarod almost until it reached the maximum speed. Therefore, to make the task more challenging, we conducted two additional rotarod trials at a five times greater rate of acceleration (Fig. 6*B*). During these trials at the faster acceleration rate, neurexin-1α KO mice continued to remain on the rotarod significantly longer than WT mice. Thus, although neurexin-1α KO mice do not display changes in

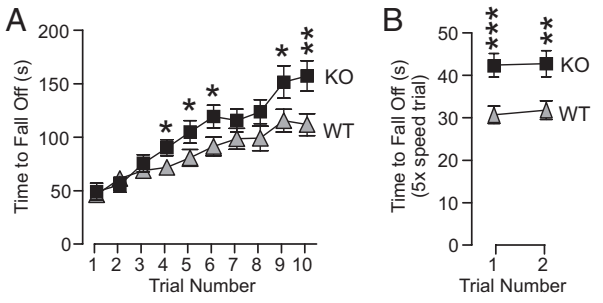

Fig. 6. Neurexin-1α KO mice exhibit enhanced motor learning on the rotarod. (*A*) Mean time WT and neurexin-1α KO mice stay on an accelerating rotarod (4–45 rpm in 5 min). Mice were tested in 10 trials, with four trials per day with a 45–60 min intertrial interval over 3 days. The time to either fall off the rod or turn one full revolution was measured. (*B*) After the experiments described in *A*, mice were subjected to an additional two trials with a higher acceleration rate (4–45 rpm in 1 min) to test the improved performance of the KO mice. Data shown are means ± SEMs (*, $P < 0.05$; **, $P < 0.01$; and ***, $P < 0.001$ compared with WT; for a full description of statistical tests and results, see *SI Appendix*).

spatial learning, they exhibit an improved capacity for motor learning.

Discussion

In the present study, we performed a parallel characterization of the electrophysiological and behavioral phenotype of neurexin-1α KO mice. We find that these mice exhibit a discrete electrophysiological phenotype, consistent with a network disruption that presents as a presynaptic loss of synaptic strength in excitatory synapses of the hippocampus (Figs. 1 and 2). This result extends previous studies showing that α-neurexin deletions produce a primarily presynaptic phenotype (9). Interestingly, the decrease in the excitatory to inhibitory balance in the neurexin-1α KO mice is yet another example of decreased excitatory/inhibitory balance in a genetic mouse model relevant to autism (38, 39). We also find that the neurexin-1α KO mice display a distinct behavioral phenotype that is consistent in part with cognitive impairments observed in ASDs and schizophrenia, which have been associated with heterozygous deletions of neurexin-1α (14–24). In addition, the moderate extent of the phenotype we observe is in agreement with the viability of neurexin-1α KO mice, the fact that other α-neurexins are still expressed in neurexin-1α KO mice, and the observation that human patients containing a heterozygous deletion of neurexin-1α are overall functional (14–24). Although the phenotype of the neurexin-1α KO mice is limited, it should be noted that some of the changes we observed are quite dramatic, as discussed below.

The neurexin-1α KO mice showed normal anxiety-related behaviors, locomotor activity, and spatial learning and memory. Their motor learning abilities were significantly enhanced. As measured on the accelerating rotarod, the KO mice learned to stay on the rod at high rotation speeds faster than littermate WT control mice. Thus, the neurexin-1α KO mice are not globally impaired; if anything, they appear rather normal in these measures of mouse behavior. On the background of this apparent normality, the three major behavioral impairments that we observed are remarkable. (*i*) We detected a large increase in repetitive grooming behaviors, indicating an abnormality with face validity to one of the three major symptom domains relevant to autism (31, 40). (*ii*) We measured a decrease in PPI, suggesting impaired sensorimotor gating. From a schizophrenia standpoint, this is an intriguing finding, because several studies have demonstrated impaired PPI in human patients with schizophrenia (28, 41–43). Similarly, impaired auditory PPI has been demonstrated in autistic patients (26, 27). (*iii*) We found an impairment in nest-building behaviors; the neurexin-1α KO mice, despite their able motor-coordination, did not expand the size of their nest. Although not straightforward to interpret, this impairment is consistent with discrete changes in organized behavior without an overall loss of brain performance.

However, we were surprised that neurexin-1α KO and WT mice exhibited virtually identical social behaviors in a number of tasks. Because impairments in social interactions are a core symptom of ASDs, neurexin-1α KO mice are of limited value as a mouse model for social dysfunction in ASDs, but they might prove useful to better understand the mechanisms underlying abnormalities in repetitive behavior that are associated with autism and ASDs (and possibly with obsessive/compulsive disorder). Also, neurexin-1α KO mice may be useful as a mouse model for sensorimotor gating deficits in schizophrenia, considering the utility of the PPI phenotype as an assay for testing therapeutic efficacy of model drugs in schizophrenics.

A major challenge in neuroscience is to relate a behavior to a particular synaptic event. Major progress has been made in this respect in the acquisition of declarative memory via the hippocampus, where long-term synaptic plasticity has been convincingly implicated (44), and a vast amount of information

exists about what brain areas are involved in specific behaviors (45). However, for most other behaviors, no information is available about the synaptic events that are involved. Thus, it is not surprising that there is a huge gap between behavioral and electrophysiological observations in mutant mice. Specifically, mutant mice frequently exhibit large behavioral changes that are difficult to relate to specific electrophysiological changes, and vice versa. Startle amplitude and PPI abnormalities, for example, can be linked to dysfunction of modulatory brain regions that are not part of the brainstem startle response circuitry (46), whereas even less is understood about the neural circuitry underlying more complex behaviors such as nesting. Also, and maybe even more importantly, many mice carrying mutations that are linked to a particular disease in human patients exhibit only parts of the disease phenotype, as observed for Rett syndrome, fragile X-syndrome, Alzheimer's disease, and Parkinson's disease mice (39, 47–50). Needless to say, this problem is particularly challenging for cognitive diseases, because many of their symptoms (e.g., the language disabilities in ASD patients or the hallucinations in schizophrenia patients) cannot even be tested in mice. In view of these limitations, painstakingly careful characterizations of electrophysiological and behavioral phenotypes of mouse models for human disorders assume an increased importance, even if a precise correlation between mouse models and human patients cannot be achieved.

Methods

Electrophysiology recordings were performed essentially as described (38) using acute hippocampal slices for extracellular (0.4 mm) and whole-cell (0.3 mm) recordings (51). Excitatory synaptic events were measured in 50 μM picrotoxin, and inhibitory events in 20 μM 6-cyano-7-nitroquinoxaline-2,3-dione and 50 μM 2-amino-5-phosphonovaleric acid. All mini recordings were performed in 0.5 μM TTX (Fig. 1), and same-cell spontaneous miniature excitatory and inhibitory events without pharmacological blockers except for 0.5 μM TTX (52). Statistical significance of data were evaluated using a Student's *t* test (for pairwise comparisons) or a Kolmogorov–Smirnov test (for cumulative probability plots). All experiments and analyses were conducted with the experimenter blind to the genotype. For detailed information, see *SI Appendix*.

Behavioral Overview. All mice tested were sex-matched, littermate progeny of matings between heterozygous neurexin-1α KO mice, and purposely maintained on a hybrid SV129/C57 black6 background to avoid artifactual phenotypes caused by mutations in homozygous inbred strains. Behavioral tests were performed on a cohort of 8 female and 12 male age- and sex-matched littermate pairs. All mice were born within 10 weeks of each other. Behaviors were tested at 2–6 months of age by experimenters blind to genotype in the following order: elevated plus maze, open field, locomotor activity (short-term locomotor habituation), grooming, social interaction with a juvenile (social learning), reciprocal social interaction with an adult conspecific, social interaction with an adult caged conspecific, 3-box social vs. inanimate preference test, rotarod, locomotor habituation in the open field (long-term locomotor habituation), interaction with pheromones, olfactory food finding, PPI, startle reactivity, Morris water maze, visible water maze, and nesting behavior. For detailed information and numerical statistical tests, see *SI Appendix*.

PPI and startle reactivity tests (53) began with six presentations of a 120 dB pulse to calculate the initial startle response (Fig. 3*A*). Afterward, the 120 dB pulse alone, prepulse/pulse pairings of 4, 8, or 16 dB above 70 dB background followed by the 120 dB pulse with a 100 ms onset-onset interval, or no stimulus were presented in pseudorandom order (Fig. 3*C*) (54). For the startle reactivity test, eight presentations of six trial types were presented in pseudorandom order: No Stimulus or 80, 90, 100, 110, or 120 dB pulses (Fig. 3*B*). Mean startle amplitudes for each condition were averaged.

Grooming Behavior. Self-grooming behavior was measured essentially as described (55, 56). Mice were habituated for 10 min in red light in an empty cage without bedding. Then, grooming of all body regions was observed for 10 min by a trained observer with a stopwatch (Fig. 4).

Social Behavior. A range of social interaction tests were performed as described (see *SI Appendix*) (38, 53, 57–60). These tests included interactions of free-moving and caged mice, and measurements of preferences for novel unfamiliar mice vs. inanimate objects (*SI Appendix*).

Nesting Behavior. After mice had habituated for 15 min in a novel empty cage, a 5 $\times$ 5 cm square of pressed cotton (Nestlet; Ancare) was placed in a random cage corner, and the net increase in nest width and next height were measured after 30, 60, and 90 min (Fig. 5).

Anxiety-Like Behaviors. The open field and elevated plus maze tests were performed essentially as described (38, 61), except that behavior was recorded by Topscan videotracking software (Version 2.0, CleverSys; *SI Appendix*).

Locomotor Activity and Habituation Behaviors were measured as described in open field or a novel empty cage (*SI Appendix*) (38, 61).

Morris water maze was conducted as described (38, 61), except that mice were given two blocks of training per day, one in the morning and one in the afternoon (*SI Appendix*).

Accelerating rotarod tests were conducted essentially as described (38, 60), except that four trials per day (with a 45–60 min intertrial interval) were conducted over 3 days. Rotarods were accelerated from 4–45 rpm in 300 s for the first 10 trials (Fig. 6*A*), and in 60 s for the last two trials (Fig. 6*B*). The time to either fall off the rod or turn one full revolution was measured.

Statistical Analysis. All statistical analysis of behavioral data were conducted using Statistica software (Version 5.5, StatSoft) using either two-way ANOVAs or three-way repeated measures ANOVAs, as appropriate (*SI Appendix*).

ACKNOWLEDGMENTS. We thank Ms. Lin Fan and Mr. Nirav Das for excellent technical assistance. This work was supported by the NIMH Grants R37 MH52804-08 (to T.C.S.) and R01 MH081164 (to C.M.P.), the Simons Foundation (to T.C.S.), the Hartwell Foundation, the BRAINS for Autism/Debra Caudy and Clay Heighten-Founders, and the Crystal Charity Ball (to C.M.P.).

1. Ushkaryov YA, Petrenko AG, Geppert M, Südhof TC (1992) Neurexins: Synaptic cell surface proteins related to the α-latrotoxin receptor and laminin. *Science* 257:50–56.
2. Ushkaryov YA, Südhof TC (1993) Neurexin IIIα: Extensive alternative splicing generates membrane-bound and soluble forms in a novel neurexin. *Proc Natl Acad Sci USA* 90:6410–6414.
3. Ushkaryov YA, et al. (1994) Conserved domain structure of ß-Neurexins. *J Biol Chem* 269:11987–11992.
4. Ichtchenko K, et al. (1995) Neuroligin 1: A splice-site specific ligand for ß-neurexins. *Cell* 81:435–443.
5. Ichtchenko K, Nguyen T, Südhof TC (1996) Structures, alternative splicing, and neurexin binding of multiple neuroligins. *J Biol Chem* 271:2676–2682.
6. Tabuchi K, Südhof TC (2002) Structure and evolution of the neurexin genes: Insight into the mechanism of alternative splicing. *Genomics* 79:849–859.
7. Rowen L, et al. (2002 Apr) Analysis of the human neurexin genes: Alternative splicing and the generation of protein diversity. *Genomics* 79:587–597.
8. Ullrich B, Ushkaryov YA, Südhof TC (1995) Cartography of neurexins: More than 1000 isoforms generated by alternative splicing and expressed in distinct subsets of neurons. *Neuron* 14:497–507.
9. Missler M, et al. (2003) α-Neurexins Couple Ca^{2+}-Channels to Synaptic Vesicle Exocytosis. *Nature* 423:939–948.
10. Kattenstroth G, Tantalaki E, Südhof TC, Gottmann K, Missler M (2004) Postsynaptic N-methyl-D-aspartate receptor function requires α-neurexins. *Proc Natl Acad Sci USA* 101:2607–2612.
11. Zhang W, et al. (2005) Extracellular domains of α-neurexins participate in regulating synaptic transmission by selectively affecting N- and P/Q-type Ca^{2+} -channels. *J Neurosci* 25:4330–4342.
12. Sons MS, et al. (2006) α-Neurexins are required for efficient transmitter release and synaptic homeostasis at the mouse neuromuscular junction. *Neuroscience* 138:433–446.
13. Dudanova I, Tabuchi K, Rohlmann A, Südhof TC, Missler M (2007) Deletion of α-Neurexins Does Not Cause a Major Impairment of Axonal Pathfinding or Synapse Formation. *J Comp Neurol* 502:261–274.
14. Szatmari P, et al. (2007) Mapping autism risk loci using genetic linkage and chromosomal rearrangements. *Nat Genet* 39:319–328.
15. Kim HG, et al. (2008) Disruption of neurexin 1 associated with autism spectrum disorder. *Am J Hum Genet* 82:199–207.
16. Yan J, et al. (2008) Neurexin α structural variants associated with autism. *Neurosci Lett* 438:368–370.
17. Sebat J, et al. (2007) Strong association of de novo copy number mutations with autism. *Science* 316:445–449.
18. Marshall CR, et al. (2008) Structural variation of chromosomes in autism spectrum disorder. *Am J Hum Genet* 82:477–488.
19. Glessner JT, et al. (2009) Autism genome-wide copy number variation reveals ubiquitin and neuronal genes. *Nature* 459:569–573.
20. Bucan M, et al. (2009) Genome-wide analyses of exonic copy number variants in a family-based study point to novel autism susceptibility genes. *PLoS Genet* 5:e1000536.

21. Zahir FR, et al. (2008) A patient with vertebral, cognitive and behavioural abnormalities and a de novo deletion of NRXN1alpha. *J Med Genet* 45:239–243.
22. Kirov G, et al. (2008) Comparative genome hybridization suggests a role for NRXN1 and APBA2 in schizophrenia. *Hum Mol Genet* 17:458–465.
23. Walsh T, et al. (2008) Rare structural variants disrupt multiple genes in neurodevelopmental pathways in schizophrenia. *Science* 320:539–543.
24. Rujescu D, et al. (2009) Disruption of the neurexin 1 gene is associated with schizophrenia. *Hum Mol Genet* 18:988–996.
25. Südhof TC (2008) Neuroligins and Neurexins Link Synaptic Function to Cognitive Disease. *Nature* 455:903–911.
26. McAlonan GM, et al. (2002) Brain anatomy and sensorimotor gating in Asperger's syndrome. *Brain* 125:1594–1606.
27. Perry W, Minassian A, Lopez B, Maron L, Lincoln A (2007) Sensorimotor gating deficits in adults with autism. *Biol Psychiatry* 61:482–486.
28. Braff DL, Geyer MA, Swerdlow NR (2001) Human studies of prepulse inhibition of startle: Normal subjects, patient groups, and pharmacological studies. *Psychopharm* 156:234–258.
29. Swerdlow NR, Braff DL, Geyer MA (2000) Animal models of deficient sensorimotor gating: What we know, what we think we know, and what we hope to know soon. *Behav Pharmacol* 11:185–204.
30. Geyer MA, McIlwain KL, Paylor R (2002) Mouse genetic models for prepulse inhibition: An early review. *Mol Psychiatry* 7:1039–1053.
31. APA (2000) *Diagnostic and Statistical Manual of Mental Disorders (DSM-IV-TR)* (American Psychiatric Association, Washington, DC).
32. Kanner L (1968) Autistic disturbances of affective contact. *Acta Paedopsychiatr* 35:100–136.
33. Lord C, Cook EH, Leventhal BL, Amaral DG (2000) Autism spectrum disorders. *Neuron* 28:355–363.
34. Crawley JN (2007) Mouse behavioral assays relevant to the symptoms of autism. *Brain Pathol* 17:448–459.
35. Lijam N, et al. (1997) Social interaction and sensorimotor gating abnormalities in mice lacking Dvl1. *Cell* 90:895–905.
36. Peripato AC, Cheverud JM (2002) Genetic influences on maternal care. *Am Nat* 160:S173–S185.
37. Blundell J, et al. (2008) Increased Anxiety-like Behavior in Mice Lacking the Inhibitory Synapse Cell Adhesion Molecule Neuroligin 2. *Genes Brain Behav* 8:114–126.
38. Tabuchi K, et al. (2007) A Neuroligin-3 Mutation Implicated in Autism Increases Inhibitory Synaptic Transmission in Mice. *Science* 318:71–76.
39. Chahrour M, Zoghbi HY (2007) The story of Rett syndrome: From clinic to neurobiology. *Neuron* 56:422–437.
40. Crawley JN (2007) Mouse behavioral assays relevant to the symptoms of autism. *Brain Pathology* 17:448–459.
41. Braff D, et al. (1978) Prestimulus effects on human startle reflex in normals and schizophrenics. *Psychophysiology* 15:339–343.
42. Braff DL, Grillon C, Geyer MA (1992) Gating and habituation of the startle reflex in schizophrenic patients. *Arch Gen Psychiatry* 49:206–215.
43. Grillon C, Ameli R, Charney DS, Krystal J, Braff D (1992) Startle gating deficits occur across prepulse intensities in schizophrenic patients. *Biol Psychiatry* 32:939–943.
44. Kandel ER (2001) The molecular biology of memory storage: A dialogue between genes and synapses. *Science* 294:1030–1038.
45. Hyman SE (2007) Can neuroscience be integrated into the DSM-V? *Nat Rev Neurosci* 8:725–732.
46. O'Donnell WT, Warren ST (2002) A decade of molecular studies of fragile X syndrome. *Annu Rev Neurosci* 25:315–338.
47. Swerdlow NR, Geyer MA, Braff DL (2001) Neural circuit regulation of prepulse inhibition of startle in the rat: Current knowledge and future challenges. *Psychopharm* 156:194–215.
47. Wong PC, Cai H, Borchelt DR, Price DL (2002) Genetically engineered mouse models of neurodegenerative diseases. *Nat Neurosci* 5:633–639.
48. Beglopoulos V, Shen J (2004) Gene-targeting technologies for the study of neurological disorders. *Neuromol Med* 6:13–30.
49. Moore DJ, Dawson TM (2007) Value of genetic models in understanding the cause and mechanisms of Parkinson's disease. *Curr Neurol Neurosci Rep* 8:288–296.
50. Volk LJ, Pfeiffer BE, Gibson JR, Huber KM (2007) Multiple Gq-coupled receptors converge on a common protein synthesis-dependent long-term depression that is affected in fragile X syndrome mental retardation. *J Neurosci* 27:11624–11634.
51. Dani VS, et al. (2005) Reduced cortical activity due to a shift in the balance between excitation and inhibition in a mouse model of Rett syndrome. *Proc Natl Acad Sci USA* 102:12560–12565.
52. Kwon CH, et al. (2006) Pten regulates neuronal arborization and social interaction in mice. *Neuron* 50:377–388.
53. Geyer MA, Dulawa SC (2003) Assessment of murine startle reactivity, prepulse inhibition, and habituation. *Current Protocols in Neuroscience* (John Wiley & Sons, Somerset, NJ), Chap 8, Unit 8:17.
54. McFarlane HG, et al. (2008) Autism-like behavioral phenotypes in BTBR T+tf/J mice. *Genes Brain Behav* 7:152–163.
55. Yang M, Zhodzishsky V, Crawley JN (2007) Social deficits in BTBR T+tf/J mice are unchanged by cross-fostering with C57BL/6J mothers. *Int J Dev Neurosci* 25:515–521.
56. Kogan JH, Frankland PW, Silva AJ (2000) Long-term memory underlying hippocampus-dependent social recognition in mice. *Hippocampus* 10:47–56.
57. Moy SS, et al. (2004) Sociability and preference for social novelty in five inbred strains: An approach to assess autistic-like behavior in mice. *Genes Brain Behav* 3:287–302.
58. Spencer CM, Alekseyenko O, Serysheva E, Yuva-Paylor LA, Paylor R (2005) Altered anxiety-related and social behaviors in the Fmr1 knockout mouse model of fragile X syndrome. *Genes Brain Behav* 4:420–430.
59. Winslow JT (2003) Mouse social recognition and preference. *Current Protocols in Neuroscience* (John Wiley & Sons, Somerset, NJ), Chap 8, Unit 8:16.
60. Powell CM, et al. (2004) The Presynaptic Active Zone Protein RIM1α is Critical for Normal Associative Learning. *Neuron* 42:143–153.